

Waveform Design and Scheduling in Space-Time Adaptive Radar

Pawan Setlur and Natasha Devroye
Electrical and Computer Engineering
University of Illinois at Chicago
Chicago, IL 60607

Muralidhar Rangaswamy
US Air Force Research Laboratory
Sensors Directorate, RYAP
WPAFB, OH 45433

Abstract—Waveform design and waveform scheduling are addressed in the context of space time adaptive processing (STAP) for radar. An air-borne radar with an array of sensors is assumed, which interrogates ground based targets. The designed waveform is assumed to be transmitted over one coherent processing interval (CPI). The waveform design and waveform scheduling problems are formulated with a cost function similar to the Minimum Variance Distortionless Response (MVDR) cost function as in classical radar STAP. Least-squared solutions for the designed waveform are obtained. It is shown that both the designed waveform and the scheduled waveforms will depend on the spatial and Doppler responses of the desired target; in particular, its spatial and temporal steering vectors. The focus of this paper will be the performance of the designed and scheduled waveforms for unknown correlation matrices but estimated from the training data, and will be addressed via simulations.

I. INTRODUCTION

The objective of this paper is to address waveform design and waveform scheduling via space time adaptive processing (STAP) in radar [1]–[5]. An air-borne radar is assumed with an array of sensor elements observing a moving target on the ground. We will assume that the waveform design and scheduling are performed over one CPI rather than on an individual pulse repetition interval (PRI).

Traditional STAP involves multidimensional adaptive filtering which combines signals from several antenna elements and from multiple waveform repetitions to suppresses clutter, interference and noise [2] in both space and time. Although detection is not the focus here, it is well known that STAP improves detection of targets in both mainlobe and sidelobe clutter and in jamming interference environments [1]–[4].

To facilitate waveform design and scheduling, we develop a STAP model considering the fast time samples along with the slow time processing. This is different from traditional STAP which generally considers the data after matched filtering [1], [2]. Nonetheless STAP research efforts have been proposed which consider inclusion of fast time samples in space time processing, see for example [1], [6], [7] and references therein. It is shown that by spatio-temporal processing prior to matched filtering, the spatio-temporal steering vector is also a function of the waveform transmitted. The minimum variance distortionless response (MVDR) optimization problem [8] for STAP seeks to minimize the undesired response from noise, clutter and interference while simultaneously preserving the target response [1]–[4].

In line with traditional STAP, we formulate both the waveform design, and the waveform scheduling problem as an MVDR type optimization. The noise, clutter, and interference are modeled stochastically and are assumed to be mutually uncorrelated. Clutter is assumed from ground reflections and hence is assumed to be persistent in most range gates. The clutter correlation matrix is a function of the waveform, and the correlation matrix of the combined noise, interference and clutter is hence also a function of the waveform transmitted. In this case, a closed form solution to the waveform design problem is not tractable. For simplicity in the analysis, we ignore the dependency of the waveform in the clutter correlation matrix, and derive a suboptimal least square (LS) solution. Not surprisingly then, it is then shown that both the waveform design and scheduling criteria depend on the spatial and temporal steering vectors of the desired target.

The paper is organized as follows: the model utilizing the fast time as well as slow time is presented in Section II. The waveform design and scheduling problems are formulated in Section III, simulations are presented in Section IV. In Section V, the conclusions are drawn based on the analysis and simulations.

In practice, the designed and scheduled waveforms will depend on the correlation matrices of noise, interference and clutter which are unknown. The major focus of this paper is to investigate the impact of using the estimated correlation matrix from training data to examine the performance loss, and will be addressed in the Section IV.

II. STAP MODEL

The radar consists of an air-borne linear array comprising M sensor elements. Without loss of generality, assume that the first sensor in the array is the phase center, and acts as both a transmitter and receiver, the rest of the elements are purely receivers. Further assume that the array is calibrated and each element in the array has an identical antenna pattern. The first sensor is located at $\mathbf{x}_r \in \mathbb{R}^3$ and the ground based point target at $\mathbf{x}_t \in \mathbb{R}^3$. The radar transmits the burst of pulses:

$$u(t) = \sum_{l=1}^L s(t - lT_p) \exp(j2\pi f_o(t - lT_p)), t \in [0, T] \quad (1)$$

where, f_o is the carrier frequency, and $T_p = 1/f_p$ is the inverse of the pulse repetition frequency, f_p . The pulse width is denoted as $T = 1/B$ and is the inverse of the bandwidth, B . Hence the coherent processing interval (CPI) consists of L pulses, each of width equal to T . The geometry of the scene is shown in Fig. 1, where θ_t and ϕ_t denote the azimuth and elevation, both of which will be useful subsequently when introducing the spatial steering vector. The radar and target are both assumed to be moving.

To develop the model, we ignore the noise, clutter and interference for the time being and assume a non-fluctuating target. Then the desired target's received signal for the l -th pulse, and at the m -th sensor element is given by

$$s_{ml}(t) = \rho_t s(t - lT_p - \tau_m) \exp(j2\pi(f_o + f_{dm})(t - lT_p - \tau_m)) \quad (2)$$

where the target's observed Doppler shift is denoted as f_{dm} , and its complex back-scattering coefficient as ρ_t . Assume that the array is along the local x axis as shown in Fig. 1. Then, the coordinates of the m -th element is given by $\mathbf{x}_t + m\mathbf{d}$, $\mathbf{d} := [d, 0, 0]^T$, $m = 0, 1, 2, \dots, M-1$, where d is the inter-element spacing. The delay τ_m could be re-written as

$$\begin{aligned} \tau_m &= \|\mathbf{x}_r - \mathbf{x}_t\|/c + \|\mathbf{x}_r + m\mathbf{d} - \mathbf{x}_t\|/c \\ &= \frac{\|\mathbf{x}_r - \mathbf{x}_t\|}{c} + \frac{\|\mathbf{x}_r - \mathbf{x}_t\|}{c} \sqrt{1 + \frac{\|\mathbf{m}\mathbf{d}\|^2}{\|\mathbf{x}_r - \mathbf{x}_t\|^2} + \frac{2m\mathbf{d}^T(\mathbf{x}_r - \mathbf{x}_t)}{\|\mathbf{x}_r - \mathbf{x}_t\|^2}} \\ &\stackrel{(a)}{=} \frac{\|\mathbf{x}_r - \mathbf{x}_t\|}{c} + \frac{\|\mathbf{x}_r - \mathbf{x}_t\|}{c} \left(1 + \frac{m\mathbf{d}^T(\mathbf{x}_r - \mathbf{x}_t)}{\|\mathbf{x}_r - \mathbf{x}_t\|^2}\right) \\ &= 2\frac{\|\mathbf{x}_r - \mathbf{x}_t\|}{c} + \frac{m\mathbf{d}^T(\mathbf{x}_r - \mathbf{x}_t)}{c\|\mathbf{x}_r - \mathbf{x}_t\|}, \end{aligned} \quad (3)$$

where in approximation (a), the term $\propto \|\mathbf{m}\mathbf{d}\|^2$ was ignored, i.e. it is assumed that $d/\|\mathbf{x}_r - \mathbf{x}_t\| \ll 1$, and then a binomial approximation was employed. It is useful now to introduce the azimuth and elevation angles, where, by geometric manipulations, we have:

$$\frac{\mathbf{x}_r - \mathbf{x}_t}{\|\mathbf{x}_r - \mathbf{x}_t\|} = [\sin(\phi_t) \sin(\theta_t), \sin(\phi_t) \cos(\theta_t), \cos(\phi_t)]^T.$$

Using the above equation in (4), the delay τ_m , $m = 0, 1, \dots, M-1$ can be rewritten as

$$\tau_m = 2\frac{\|\mathbf{x}_r - \mathbf{x}_t\|}{c} + \frac{md \sin(\phi_t) \sin(\theta_t)}{c}. \quad (5)$$

The Doppler shift, i.e. f_{dm} is computed as

$$\begin{aligned} f_{dm} &= 2f_o \frac{(\dot{\mathbf{x}}_r - \dot{\mathbf{x}}_t)^T(\mathbf{x}_r - \mathbf{x}_t)}{c\|\mathbf{x}_r - \mathbf{x}_t\|} \\ &+ f_o \frac{m\mathbf{d}^T}{c} \left[\frac{\dot{\mathbf{x}}_r - \dot{\mathbf{x}}_t}{\|\mathbf{x}_r - \mathbf{x}_t\|^2} - \frac{(\mathbf{x}_r - \mathbf{x}_t)(\dot{\mathbf{x}}_r - \dot{\mathbf{x}}_t)^T(\mathbf{x}_r - \mathbf{x}_t)}{\|\mathbf{x}_r - \mathbf{x}_t\|^3} \right] \end{aligned} \quad (6)$$

where $\dot{\mathbf{x}}_{(\cdot)}$ is the vector differential of $\mathbf{x}_{(\cdot)}$ w.r.t time. In practice d is a fraction of the wavelength, and assuming that $d/\|\mathbf{x}_r - \mathbf{x}_t\| \ll 1$ we approximate the second term in (6) as 0. The Doppler shift is no longer a function of the sensor

index, m , and is rewritten as

$$f_{dm} = f_d = 2f_o \frac{(\dot{\mathbf{x}}_r - \dot{\mathbf{x}}_t)^T(\mathbf{x}_r - \mathbf{x}_t)}{c\|\mathbf{x}_r - \mathbf{x}_t\|} \quad (7)$$

Assumption A1: From here onwards, the standard narrow-band assumption is invoked [1], i.e. the signal propagation time across the array is assumed to be much smaller than the inverse of the signal bandwidth. This then implies that $s(t - 2\|\mathbf{x}_r - \mathbf{x}_t\|/c - md \sin(\phi_t) \sin(\theta_t)/c) \approx s(t - 2\|\mathbf{x}_r - \mathbf{x}_t\|/c)$. Using this and substituting (5) and (7) in (2), and downconverting to baseband we obtain,

$$\begin{aligned} s_{ml}(t) &= \rho_t s(t - lT_p - \tau_t) e^{-j4\pi(f_o + f_d)\tau_t} e^{-j2\pi \frac{md \sin(\phi_t) \sin(\theta_t)}{\lambda_o}} \\ &\times e^{-j2\pi f_d \frac{md \sin(\phi_t) \sin(\theta_t)}{c}} e^{j2\pi f_d (t - lT_p)} \end{aligned} \quad (8)$$

where $\tau_t = 2\|\mathbf{x}_r - \mathbf{x}_t\|/c$ and λ_o is the operating wavelength. Some practical approximations can now be made on (8).

Assumption A2: For arguments sake let $d = \lambda_o/p$, where p is an arbitrary positive integer ($p = 2$ is the critical spatial Nyquist). Then,

$$\exp(-j2\pi f_d \frac{md \sin(\phi_t) \sin(\theta_t)}{c}) = \exp(-j2\pi \frac{mf_d \sin(\phi_t) \sin(\theta_t)}{pf_o}) \approx 1$$

It is easily shown that this assumption is valid in most general cases. However, this is invalidated for long array apertures ($M > 100$), which in the first place could be impractical for air-borne radar systems.

Assumption A3: We assume that the phase from the Doppler is insignificant within the fast time, i.e. t . In other words, we assume that $\exp(j2\pi f_d t) \approx 1$, $t \in [0, T]$. For practical Doppler shifts this is reasonable.

These assumptions are now enforced in (8), without explicitly stating them in the rest of the paper. Examples validating A1-A3 are subsequently discussed in Section II-B.

A. Vector signal model

Let $s(t)$ be sampled discretely resulting in N discrete time samples. Consider for now the single range gate corresponding to the time delay τ_t . Then after a suitable alignment to a common local time (or range) reference, (8) may be rewritten in a vector defined as $\mathbf{y}_l \in \mathbb{C}^{NM}$, and given by

$$\mathbf{y}_l = \rho_t \mathbf{s} \otimes \mathbf{a}(\theta_t, \phi_t) \exp(-j2\pi f_d l T_p) \quad (9)$$

$$\mathbf{s} := [s(0), s(1), \dots, s(N-1)]^T \in \mathbb{C}^N$$

$$\mathbf{a}(\theta_t, \phi_t) := [1, e^{-j2\pi\vartheta}, e^{-j4\pi\vartheta}, \dots, e^{-j2\pi(M-1)\vartheta}]^T \in \mathbb{C}^M$$

where $\vartheta := d \sin(\theta_t) \sin(\phi_t)/\lambda_o$ is defined as the spatial frequency. Further it is noted that in (9), the constant phase terms have been absorbed into ρ_t . Considering the L pulses together, i.e. concatenating the desired target's response for the entire CPI in a tall vector \mathbf{y} , is defined as

$$\begin{aligned} \mathbf{y} &\in \mathbb{C}^{NML} = [\mathbf{y}_1^T, \mathbf{y}_2^T, \dots, \mathbf{y}_L^T]^T \\ \mathbf{y} &= \rho_t \mathbf{s} \otimes \mathbf{a}(\theta_t, \phi_t) \otimes \mathbf{v}(f_d) \\ \mathbf{v}(f_d) &:= [1, e^{-j2\pi f_d T_p}, e^{-j4\pi f_d T_p}, \dots, e^{-j2\pi f_d (L-1)T_p}]^T \end{aligned} \quad (10)$$

The vector \mathbf{y} consists of both the spatial and the temporal steering vectors as in classical STAP, as well as the waveform dependency, via waveform vector \mathbf{s} .

At the considered range gate, the measured snapshot vector consists of the target returns and the undesired returns, i.e. clutter returns, interference and noise. The contaminated snapshot at the considered range gate is then given by

$$\begin{aligned}\bar{\mathbf{y}} &= \mathbf{y} + \mathbf{y}_i + \mathbf{y}_c + \mathbf{y}_n \\ &= \mathbf{y} + \mathbf{y}_u\end{aligned}\quad (11)$$

where $\mathbf{y}_i, \mathbf{y}_c, \mathbf{y}_n$ are the contributions from the interference, clutter and noise, respectively, and are assumed to be statistically uncorrelated with one another. The contribution of the undesired returns are treated in detail, starting with the noise as it is the simplest.

Noise: The noise is assumed to be zero mean, identically distributed across the sensors, across pulses, and in the fast time samples. The correlation matrix of \mathbf{y}_n is denoted as $\mathbf{R}_n \in \mathbb{C}^{NML \times NML}$. The simplest example is when the noise is independent across the sensors, the pulses, and the fast time samples, i.e. $\mathbf{R}_n \propto \mathbf{I}$, where \mathbf{I} is the identity matrix of appropriate dimensions.

Interference: The interference consists of jammers and other intentional / un-intentional sources which may be ground based, air-borne or both. Let us assume that there are K interference sources. Further, since nothing is known about the jammers waveform characteristics, the waveform itself is assumed to be a stationary zero mean random process. Consider the k -th interference source in the l -th PRI, and at spatial co-ordinates (θ_k, ϕ_k) . Its corresponding snapshot contribution is modeled as,

$$\mathbf{y}_{kl} = \boldsymbol{\alpha}_{kl} \otimes \mathbf{a}(\theta_k, \phi_k), k = 1, 2, \dots, K, l = 1, 2, \dots, L \quad (12)$$

where $\boldsymbol{\alpha}_{kl} = [\alpha_{kl}(0), \alpha_{kl}(1), \dots, \alpha_{kl}(N-1)]^T \in \mathbb{C}^N$ is the random discrete segment of the jammer waveform, as seen by the radar in the l -th PRI. Stacking \mathbf{y}_{kl} for a fixed k as a tall vector, we have

$$\begin{aligned}\mathbf{y}_k &= \boldsymbol{\alpha}_k \otimes \mathbf{a}(\theta_k, \phi_k) \\ &= [\mathbf{y}_{k1}^T, \mathbf{y}_{k2}^T, \dots, \mathbf{y}_{kL}^T]^T \in \mathbb{C}^{NML} \\ \boldsymbol{\alpha}_k &:= [\boldsymbol{\alpha}_{k1}^T, \boldsymbol{\alpha}_{k2}^T, \dots, \boldsymbol{\alpha}_{kL}^T]^T \in \mathbb{C}^{NL}\end{aligned}\quad (13)$$

Using the Kronecker mixed product property, (see for e.g. [9]), the correlation matrix of \mathbf{y}_k is expressed as

$$\mathbb{E}\{\mathbf{y}_k \mathbf{y}_k^H\} = \mathbf{R}_\alpha^k \otimes \mathbf{a}(\theta_k, \phi_k) \mathbf{a}(\theta_k, \phi_k)^H$$

where, $\mathbb{E}\{\boldsymbol{\alpha}_k \boldsymbol{\alpha}_k^H\} := \mathbf{R}_\alpha^k$. For K mutually uncorrelated interferers, the correlation matrix is $\mathbf{R}_i = \sum_{k=1}^K \mathbb{E}\{\mathbf{y}_k \mathbf{y}_k^H\}$, and is simplified as

$$\begin{aligned}\mathbf{R}_i &= \sum_{k=1}^K \mathbf{R}_\alpha^k \otimes \mathbf{a}(\theta_k, \phi_k) \mathbf{a}(\theta_k, \phi_k)^H \\ &= \sum_{k=1}^K (\mathbf{I}_{NL} \otimes \mathbf{a}(\theta_k, \phi_k)) \mathbf{R}_\alpha^k (\mathbf{I}_{NL} \otimes \mathbf{a}(\theta_k, \phi_k))^H \\ &= \mathbf{A}(\theta, \phi) \mathbf{R}_\alpha \mathbf{A}(\theta, \phi)^H\end{aligned}\quad (14)$$

where

$$\begin{aligned}\mathbf{R}_\alpha &:= \text{Diag}\{\mathbf{R}_\alpha^1, \mathbf{R}_\alpha^2, \dots, \mathbf{R}_\alpha^K\} \in \mathbb{C}^{NMLK \times NMLK} \\ \mathbf{A}(\theta, \phi) &\in \mathbb{C}^{NML \times NMLK} \\ &:= [\mathbf{I}_{NL} \otimes \mathbf{a}(\theta_1, \phi_1), \mathbf{I}_{NL} \otimes \mathbf{a}(\theta_2, \phi_2), \dots, \mathbf{I}_{NL} \otimes \mathbf{a}(\theta_K, \phi_K)],\end{aligned}$$

for \mathbf{I}_{NL} the identity matrix of size $NL \times NL$, and $\text{Diag}\{\cdot, \cdot, \dots, \cdot\}$ the matrix diagonal operator which converts the matrix arguments into a bigger diagonal matrix. For example, $\text{Diag}\{\mathbf{A}, \mathbf{B}, \mathbf{C}\} = \begin{bmatrix} \mathbf{A} & \mathbf{0} & \mathbf{0} \\ \mathbf{0} & \mathbf{B} & \mathbf{0} \\ \mathbf{0} & \mathbf{0} & \mathbf{C} \end{bmatrix}$.

Clutter: The ground is a major source of clutter in air-borne radar applications and is persistent in all range gates upto the gate corresponding to the platform horizon. Other sources of clutter surely exist, such as buildings, trees, as well as other un-interesting targets. We will ignore the other sources of clutter and treat ground clutter stochastically.

Let us assume that there are Q clutter patches indexed by parameter q . Assume that the q -th clutter patch is at $(\theta_q, \phi_q), q = 1, 2, \dots, Q$, with a corresponding co-ordinate vector denoted as \mathbf{x}_q . Each of these clutter patches are comprised of say P scatterers. Assuming that the scatterers do not scintillate in the PRI's, the radar return from the p -th scatterer in the q -th clutter patch is given by

$$\gamma_{pq} \mathbf{s} \otimes a(\theta_q, \phi_q) \otimes \mathbf{v}(fc_q)$$

where γ_{pq} is its random complex reflectivity, and fc_q is the Doppler shift observed from the q -th clutter patch. It is implicitly assumed that the scatterers in a particular clutter patch have identical Doppler as they are in the same range gate. Furthermore, it is also implicitly assumed that due to the far-field assumptions, the scatterers are in the same azimuth resolution cell. In other words the spatial responses of scatterers in the same clutter patch are identical to one another. The Doppler fc_q is given by,

$$fc_q := \frac{2f_o \dot{\mathbf{x}}_r^T (\mathbf{x}_r - \mathbf{x}_q)}{c \|\mathbf{x}_r - \mathbf{x}_q\|}. \quad (15)$$

Since the clutter patch is stationary, the Doppler is purely from the motion of the aircraft as seen in (15). The contribution from the q -th clutter patch to the received signal is given by

$$\mathbf{y}_q = \sum_{p=1}^P \gamma_{pq} \mathbf{s} \otimes a(\theta_q, \phi_q) \otimes \mathbf{v}(fc_q), \quad (16)$$

with corresponding correlation matrix

$$\mathbf{R}_\gamma^q := \mathbf{B}_q \mathbf{R}_\gamma^{pq} \mathbf{B}_q^H \quad (17)$$

where, $\mathbf{B}_q = [\mathbf{s} \otimes \mathbf{a}(\theta_q, \phi_q) \otimes \mathbf{v}(fc_q), \dots, \mathbf{s} \otimes \mathbf{a}(\theta_q, \phi_q) \otimes \mathbf{v}(fc_q)] \in \mathbb{C}^{NML \times P}$ and \mathbf{R}_γ^{pq} is the correlation matrix of the random vector, $[\gamma_{1q}, \gamma_{2q}, \dots, \gamma_{Pq}]^T$. Assuming that a particular scatterer from one clutter patch is uncorrelated to any other scatterer belonging to any other clutter patch, we have the net contribution of clutter $\mathbf{y}_c = \sum_{q=1}^Q \mathbf{y}_q$, with

corresponding correlation matrix given by

$$\mathbf{R}_c = \sum_{q=1}^Q \mathbf{R}_\gamma^q. \quad (18)$$

B. Assumptions on the parameters

Assume $f_o = 10$ GHz, $B = 1/T = 50$ MHz, $M = 10$, $\theta_t = 60^\circ$, $\phi_t = 40^\circ$, that the radar platform has a velocity vector given by $\dot{\mathbf{x}}_r = [100, 0, 0]^T$ m/s, likewise the target's velocity vector is $\dot{\mathbf{x}}_t = [60, 0, 0]^T$ miles per hour. Then the propagation time across the array is $4.5e-10$ assuming the inter element spacing is $\lambda_o/2$, which is clearly much less than the inverse of the bandwidth. Hence the narrowband assumption i.e. A1 is satisfied. Using these values of the radar parameters, we obtain the target Doppler, $f_d = 2.713$ kHz. Substituting these values, we find that A2 is also satisfied for $p = 2, 3, \dots$. Next, we find that $\exp(j2\pi f_d T) = 1 + 0.0003j$, clearly then for $t \leq 1/B$, assumption A3 is also satisfied.

III. WAVEFORM DESIGN AND WAVEFORM SCHEDULING

The radar return at the considered range gate is processed by a filter characterized by a weight vector, \mathbf{w} , whose output is given by $\mathbf{w}^H \bar{\mathbf{y}}$. The objective of STAP is to obtain the desired \mathbf{w} such that the power from the undesired response is minimized, while leaving the target response as is. Since the waveform \mathbf{s} prominently figures in the steering vector, say for example in (10), our objective is to both design the waveform as well as obtain the desired weight vector, \mathbf{w} . Mathematically, we may formulate this problem as:

$$\begin{aligned} \min_{\mathbf{w}, \mathbf{s}} \quad & \mathbb{E}\{|\mathbf{w}^H \mathbf{y}_u|^2\} \\ \text{s. t} \quad & \mathbf{w}^H (\mathbf{s} \otimes \mathbf{a}(\theta_t, \phi_t) \otimes \mathbf{v}(f_d)) = 1 \end{aligned} \quad (19)$$

Solving (19) jointly over the optimization variables proves difficult. However, the method of concentration as applied to maximum likelihood problems, proves useful. In other words, solving the minimization problem w.r.t to \mathbf{w} by initially treating \mathbf{s} as a constant, the solution to (19) is well known, and expressed as

$$\mathbf{w}_o = \frac{\mathbf{R}_u^{-1} (\mathbf{s} \otimes \mathbf{a}(\theta_t, \phi_t) \otimes \mathbf{v}(f_d))}{(\mathbf{s} \otimes \mathbf{a}(\theta_t, \phi_t) \otimes \mathbf{v}(f_d))^H \mathbf{R}_u^{-1} (\mathbf{s} \otimes \mathbf{a}(\theta_t, \phi_t) \otimes \mathbf{v}(f_d))} \quad (20)$$

where $\mathbf{R}_u = \mathbf{R}_i + \mathbf{R}_c + \mathbf{R}_n$. We further emphasize that the the weight vector is an explicit function of the waveform. Now substituting \mathbf{w}_o back into the cost function in (19), the minimization is purely w.r.t \mathbf{s} , with the constraint already being satisfied $\forall \mathbf{s}$. In other words, the new minimization problem is unconstrained, and cast as,

$$\min_{\mathbf{s}} \frac{1}{(\mathbf{s} \otimes \mathbf{a}(\theta_t, \phi_t) \otimes \mathbf{v}(f_d))^H \mathbf{R}_u^{-1} (\mathbf{s} \otimes \mathbf{a}(\theta_t, \phi_t) \otimes \mathbf{v}(f_d))} \quad (21)$$

In the presence of clutter, which is assumed here, the correlation matrix \mathbf{R}_u is a function of \mathbf{s} , although not explicitly stated but which can be seen from say (16) and (17). In the absence of

clutter but presence of noise and interference, this is not true. Solving (21) while enforcing the dependency of \mathbf{R}_u on \mathbf{s} is intractable. Rather, a suboptimal solution ignores the implicit dependency of \mathbf{R}_u on \mathbf{s} is advocated. Then, the solution to (21) can be formulated as Rayleigh-Ritz optimization [9], resulting in the solution:

$$\mathbf{s} \otimes \mathbf{a}(\theta_t, \phi_t) \otimes \mathbf{v}(f_d) = \boldsymbol{\mu}_{\min}(\mathbf{R}_u) \quad (22)$$

where $\boldsymbol{\mu}_{\min}(\mathbf{R}_u)$ is the *eigenvector corresponding to the minimum eigenvalue of \mathbf{R}_u* . This tensor equation implicitly defines the optimal \mathbf{s} ; whether this equation may be met with equality depends on the dimensions and values of $\mathbf{a}(\theta_t, \phi_t)$, $\mathbf{v}(f_d)$, and \mathbf{R}_u . In general the system is overdetermined and we solve this equation approximately via least squares (LS) [10], as described next.

A. Waveform design solution

Define $\boldsymbol{\chi} := \mathbf{a}(\theta_t, \phi_t) \otimes \mathbf{v}(f_d) = [\chi_1, \dots, \chi_{ML}]^T$, likewise define $s_i := s(i)$ to simplify notation. Then, from (22), the following NML equations are obtained:

$$\begin{aligned} s_i \chi_j &= \mu_h, i = 1, 2, \dots, N, j = 1, 2, \dots, ML \\ h &= (i-1)ML + j \end{aligned} \quad (23)$$

where μ_h is the h -th element of vector $\boldsymbol{\mu}_{\min}(\mathbf{R}_u)$.

The system of equations in (23) may be written as a linear matrix equation,

$$\begin{aligned} \boldsymbol{\mu}_{\min}(\mathbf{R}_u) &= \mathbf{H} \mathbf{s} \\ \mathbf{H} &:= \begin{bmatrix} \boldsymbol{\chi} & \mathbf{0} & \mathbf{0} & \cdots & \mathbf{0} \\ \mathbf{0} & \boldsymbol{\chi} & \mathbf{0} & \cdots & \mathbf{0} \\ \mathbf{0} & \mathbf{0} & \boldsymbol{\chi} & \vdots & \vdots \\ \vdots & \vdots & \vdots & \vdots & \vdots \end{bmatrix} \in \mathbb{C}^{NML \times N} \end{aligned} \quad (24)$$

where $\mathbf{0}$ is a column vector of dimension N , consisting of all zeros. A LS solution is employed to solve (24), with the corresponding cost function and solution readily given by

$$\min_{\mathbf{s}} \|\boldsymbol{\mu}_{\min}(\mathbf{R}_u) - \mathbf{H} \mathbf{s}\|^2 \quad (25)$$

$$\hat{\mathbf{s}} = (\mathbf{H}^H \mathbf{H})^{-1} \mathbf{H}^H \boldsymbol{\mu}_{\min}(\mathbf{R}_u) \quad (26)$$

where $\hat{\mathbf{s}}$ is the LS estimate of \mathbf{s} . After some straightforward matrix algebra, the solution to (25) is simplified further, i.e.

$$\hat{s}_i = \frac{\boldsymbol{\chi}^H \boldsymbol{\mu}_h}{\boldsymbol{\chi}^H \boldsymbol{\chi}}, i = 1, 2, \dots, N \quad (27)$$

$$\boldsymbol{\mu}_h = [\mu_{(i-1)ML+1}, \mu_{(i-1)ML+2}, \dots, \mu_{iML}]^T \in \mathbb{C}^{ML}$$

It is readily seen that \hat{s}_i are solutions to the individual LS optimization costs, $\min_{s_i} \|\boldsymbol{\mu}_h - s_i \boldsymbol{\chi}\|^2$. In other words, the LS cost in (25) decouples into N separable LS costs. It is noted that the waveform solutions are unconstrained, the solutions will change when we put additional constraints, for example, constant modulus, which is not the focus of this paper.

In practice it is noted that the matrix \mathbf{R}_u is unknown and must be estimated from the STAP data cube shown in Fig. 2. Typically several range cells are used to estimate the

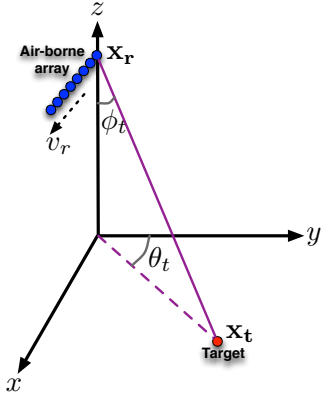


Fig. 1. Radar scene considering the ground based target at azimuth (θ_t), elevation (ϕ_t). The (x, y, z) axis are local to the aircraft carrying the array.

undesired correlation matrix which are not in the immediate vicinity of the range cell under consideration. This is done to prevent self-nulling of the hypothesized target responses from either the main lobe or via the sidelobe responses. If $\bar{\mathbf{y}}_r \in \mathbb{C}^{NML}$, $r = 1, 2, \dots, R$ denotes the radar returns from R range gates consisting of only undesired returns (target free), then the following sample matrix estimate of \mathbf{R}_u is used:

$$\hat{\mathbf{R}}_u = \sum_{r=1}^R \bar{\mathbf{y}}_r \bar{\mathbf{y}}_r^H / R \quad (28)$$

Therefore to ensure invertibility in (21), $R \geq NML$ is needed. The effect of using (28) will have an impact on the designed as well as scheduled waveforms, and is addressed in the simulations section.

Waveform scheduling: When waveform scheduling rather than design is desired, then (21) may be used directly by minimizing over the waveform library given by the set $\mathcal{S} = \{\mathbf{s}_1, \mathbf{s}_2, \dots, \mathbf{s}_U\}$. For example, if a target of interest is being tracked, then scheduling is envisioned by using the previously obtained estimate of \mathbf{R}_u from the prior CPI to schedule for the future CPI's. Typically CPI's are in the order of milliseconds (or lower). Hence it may be reasonable to assume that the correlation matrix of the undesired radar returns remain approximately stationary for a few contiguous CPIs. It is further noted that waveform design may aid in waveform scheduling, i.e. the waveform library could be made dynamic by incorporating some of the previously designed waveforms into the waveform library, on-the-fly.

IV. SIMULATIONS

In practice, the designed and scheduled waveforms will depend on the correlation matrices of noise, interference and clutter which is unknown. The major focus of this paper is to investigate the impact of using the estimated correlation matrix from training data to examine the performance loss, and is addressed via a numerical simulation.

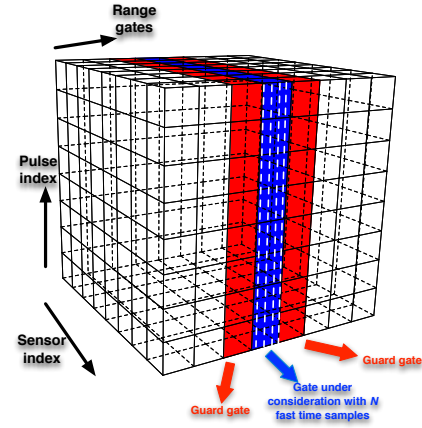


Fig. 2. STAP data cube before matched filtering or range compression, depicting the considered range gate/cell and fast time slices (dashed lines).

The noise correlation matrix was assumed to be a scaled identity matrix assuming an SNR of 20dB. The carrier frequency was chosen to be 10GHz, and the radar bandwidth was 50MHz. To reduce computation complexity in inverting large matrices and their eigen-decompositions, we considered $M = 5, L = 32, N = 5$. The element spacing i.e. $d = \lambda_o/2$. Two interference sources were considered at $(\theta = \pi/3, \phi = 5\pi/2)$ and at $(2\pi/3, 5\pi/2)$. Both these interference sources had identical discrete correlation functions given by $0.8^{|n|}$, $n = 0, 1, 2, \dots$, in other words comprising the appropriate elements in matrices \mathbf{R}_α^1 and \mathbf{R}_α^2 . The interference correlation was constructed using (14). To simulate clutter we considered two clutter patches, consisting of four scatters each. To keep the analysis simple, we assumed that the clutter scatters are uncorrelated in their respective patches as well as across them. In other words, $\mathbf{R}_\gamma^{pq} = \mathbf{I}\mathbf{V}(p, q)$. The two clutter patches were assumed to be at angle co-ordinates given by $(\theta = \pi/4, \phi = \pi/4)$ and $(2\pi/5, \pi/4)$, respectively. The velocity $\dot{\mathbf{x}}_r = [100, 0, 0]^T$. The clutter Doppler can now be computed from say (15), and the corresponding clutter correlation matrix may be computed from (18).

The loss of performance can now be computed and is defined as the ratio of the variance of the Capon using the true correlation matrix to the ratio of the variance of the capon using the estimated correlation matrix, see also [2]. To estimate the correlation, we sampled a multivariate Gaussian distribution using the true parameters, namely zero mean and correlation given by \mathbf{R}_u . Then the estimate used in (28) was used. The results are shown in 3. It is seen that to be close to the 3dB tolerance, we must have $R \geq 2NML$, to get in the proximity of 1dB to the optimal performance we need $3NML \leq R \leq 4NML$, which may be prohibitive in certain airborne applications.

V. CONCLUSIONS AND FUTURE DIRECTIONS

Waveform design and waveform scheduling were addressed for space time adaptive processing (STAP) in an airborne radar. An linear array of radar sensors was assumed, interrogating

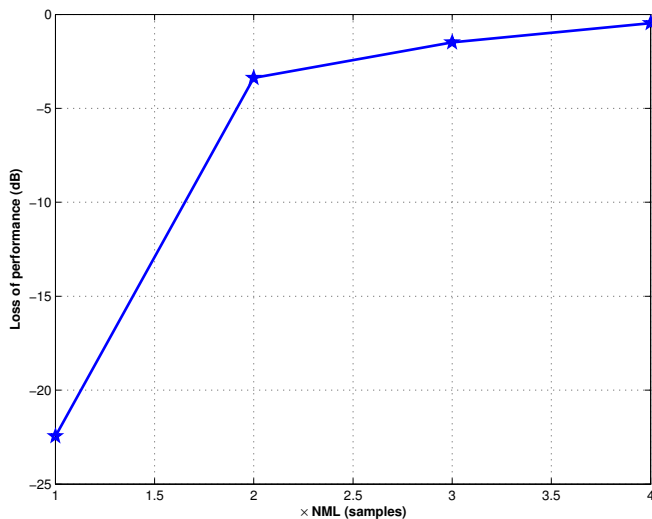


Fig. 3. Loss of performance in dBs vs samples

ground based targets. The waveform design and waveform scheduling problems were formulated with a cost function similar to the MVDR cost function as in classical radar STAP. It is shown analytically derived that both the designed waveform and the scheduled waveforms will depend on the spatial and Doppler responses of the desired target. A numerical result was shown that demonstrates that when the covariance matrix of the undesired responses are estimated, the loss of performance is inversely proportional to the number of samples used in estimation of the covariance matrix.

The analysis in this paper thus far ignored the signal dependency of the clutter correlation matrix, resulting in the well known Rayleigh-Ritz optimization problem leading to the eigenvector solution. Future directions along this line of research may include this signal dependency of clutter. Further, possible investigative directions may also include adding additional radar waveform specific constraints such as peak sidelobe levels, constant modulus, Doppler tolerance levels etc.. Nonetheless, it remains to be seen if such solutions result in minimizing the MVDR variance to appreciably lower levels than the suboptimal eigenvector solution.

ACKNOWLEDGEMENT

This work was sponsored by US AFOSR under award FA9550-10-1-0239; no official endorsement must be inferred.

REFERENCES

- [1] R. Klemm, *Principles of Space-Time Adaptive Processing*. Institution of Electrical Engineers, 2002.
- [2] J. Ward, *Space-time Adaptive Processing for Airborne Radar*, ser. Technical report (Lincoln Laboratory). Massachusetts Institute of Technology, Lincoln Laboratory, 1994.
- [3] J. Guerci, *Space-Time Adaptive Processing for Radar*. Artech House, 2003.
- [4] L. E. Brennan and L. S. Reed, "Theory of Adaptive Radar," *IEEE Transactions on Aerospace and Electronic Systems*, vol. AES-9, no. 2, pp. 237–252, Mar. 1973.

- [5] A. Farina, A. Saverione, and L. Timmoneri, "The MVDR vectorial lattice applied to space-time processing for AEW radar with large instantaneous bandwidth," *IEE Proc. Radar, Sonar and Navigation (Pt. F)*, vol. 143, no. 1, pp. 41–46, Feb. 1996.
- [6] D. Madurasinghe and A. P. Shaw, "Mainlobe jammer nulling via tsi finders: a space fast-time adaptive processor," *EURASIP J. Appl. Signal Process.*, vol. 2006, pp. 221–221, Jan. 2006.
- [7] Y. Seliktar, D. B. Williams, and E. J. Holder, "A space/fast-time adaptive monopulse technique," *EURASIP J. Appl. Signal Process.*, vol. 2006, pp. 218–218, Jan. 2006. [Online]. Available: <http://dx.doi.org/10.1155/ASP/2006/14510>
- [8] J. Capon, "High-resolution frequency-wavenumber spectrum analysis," *Proceedings of the IEEE*, vol. 57, no. 8, pp. 1408–1418, Jun. 1969.
- [9] R. Horn and C. Johnson, *Topics in Matrix Analysis*. Cambridge University Press, 1994.
- [10] G. Strang, *Linear Algebra and Its Applications*. Thomson, Brooks/Cole, 2006.